Mon. Not. R. Astron. Soc. **000**, 000–000 (0000) Printed 2 March 2013 (MN LATEX style file v2.2)

Misleading variations in estimated rotational frequency splittings of solar p modes: Consequences for helio- and asteroseismology

Anne-Marie Broomhall,[1⋆] David Salabert,[2,3,4] William J. Chaplin,[1] Rafael A. García,[5] Yvonne Elsworth,[1] Rachel Howe[1] and Savita Mathur[6]

[1]*School of Physics and Astronomy, University of Birmingham, Edgbaston, Birmingham B15 2TT*
[2]*Instituto de Astrofísica de Canarias, E-38200 La Laguna, Tenerife, Spain*
[3]*Departamento do Astrofísica, Universidad de La Laguna, E-38206 La Laguna, Tenerife, Spain*
[4]*Université de Nice Sophia-Antipolis, CNRS UMR 6202, Observatoire de la Côte dAzur, BP 4229, 06304 Nice Cedex 4, France*
[5]*Laboratoire AIM, CEA/DSM-CNRS-Université Paris Diderot, IRFU/SAp, Centre de Saclay, 91191 Gif-sur-Yvette, France*
[6]*High Altitude Observatory, NCAR, PO Box 3000, Boulder, CO 80307, USA*

ABSTRACT

The aim of this paper is to investigate whether there are any 11-yr or quasi-biennial solar cycle-related variations in solar rotational splitting frequencies of low-degree solar p modes. Although no 11-yr signals were observed, variations on a shorter timescale (~ 2 yrs) were apparent. We show that the variations arose from complications/artifacts associated with the realization noise in the data and the process by which the data were analyzed. More specifically, the realization noise was observed to have a larger effect on the rotational splittings than accounted for by the formal uncertainties. When used to infer the rotation profile of the Sun these variations are not important. The outer regions of the solar interior can be constrained using higher-degree modes. While the variations in the low-l splittings do make large differences to the inferred rotation rate of the core, the core rotation rate is so poorly constrained, even by low-l modes, that the different inferred rotation profiles still agree within their respective 1σ uncertainties. By contrast, in asteroseismology, only low-l modes are visible and so higher-l modes cannot be used to constrain the rotation profile of stars. Furthermore, we usually only have one data set from which to measure the observed low-l splitting. In such circumstances the inferred internal rotation rate of a main sequence star could differ significantly from estimates of the surface rotation rate, hence leading to spurious conclusions. Therefore, extreme care must be taken when using only the splittings of low-l modes to draw conclusions about the average internal rotation rate of a star.

Key words: Methods: data analysis, Sun: activity, Sun: helioseismology, Sun: oscillations, stars: oscillations

1 INTRODUCTION

The frequencies of the Sun's acoustic (p-mode) oscillations vary throughout the solar cycle with the frequencies of the most prominent modes being at their highest when solar activity is at its maximum (e.g. Woodard & Noyes 1985; Pallé, Régulo & Roca Cortés 1989; Elsworth et al. 1990; Salabert et al. 2004; Chaplin et al. 2007; Jiménez-Reyes et al. 2007). Mid-term signals ($\lesssim 2$ yr) can also be observed in p-mode frequencies (e.g. Broomhall et al. 2009; Salabert et al. 2009; Fletcher et al. 2010). Solar cycle variations are also observed in other p-mode parameters such as powers and lifetimes (e.g. Salabert, Jiménez-Reyes & Tomczyk 2003; Jiménez-Reyes et al. 2004). With the advent of long, continuous, and high-quality asteroseismic observations of solar-like stars (e.g. Chaplin et al. 2011) by the Convection Rotation and Planetary Transits (CoRoT; Baglin et al. 2006) space mission and Kepler (Borucki et al. 2010) it is possible to study changes in p-mode properties (García et al. 2010; Salabert et al. 2011b) and to measure rotational splittings (Ballot et al. 2011; Beck et al. 2012).

Solar rotation splits p modes into $2l + 1$ azimuthal orders (m). The difference in frequency between azimuthal orders of a mode can be used to infer the Sun's internal rotation profile. Variations in the splittings of intermediate-l modes ($5 \leq l \leq 300$) have been used to observe the torsional oscillation (Howe 2009, and references therein). No noticeable 11-yr solar cycle changes in the p-mode splittings of low-l data have been observed to date (e.g. Jiménez, Roca Cortés & Jiménez-Reyes 2002; Gelly et al. 2002; García et al. 2004, 2008; Salabert et al. 2011a). Howe et al. (2000) used the rotational splittings of medium-l p modes to infer the evolution of the rotation rate at the base of the convection zone through the solar cycle. Howe et al. found a 1.3 yr periodicity in the data, however, the signal seemed to disappear after 2000 (Howe et al. 2007). Furthermore, the result was not confirmed by other investigations (e.g. Basu & Antia 2001, 2003). Salabert et al. (2011a) observed mid-term variations in the rotational splittings of low-l modes. Here we examine whether solar cycle-related changes, potentially including mid-term

⋆ amb@bison.ph.bham.ac.uk

variations, can be observed in the most up-to-date low-l p-mode splittings. We also discuss the consequences of observed variations in the rotational splitting on solar rotation profile inversions.

Acoustic p modes are not the only oscillations that propagate through the interior of a star. Gravity (g) modes can propagate only in regions of stable stratification and so are trapped within the central regions of a star, beneath the convection zone. Mixed modes show characteristics of both p and g modes, carrying information on both the outer envelope and the central core. Mixed modes have been detected in stars that have evolved off the main sequence and the splittings of mixed modes have been used to infer the rotation rate of stellar cores (Beck et al. 2012; Deheuvels et al. 2012, and references therein). However, here we consider only the inferred average internal rotation rate of main sequence stars, like the Sun, that do not have detectible g modes and mixed modes. We must, therefore, rely on the splittings of low-l p modes only and so any variations in the splittings could be important.

The structure of this paper is as follows: In Section 2 we describe how the frequency splittings were obtained and discuss the presence of any periodicities. In Section 3 we compare the results obtained from the real data with those obtained from simulated data. In Section 4 the consequences of the variations in the splittings for inversions of the internal rotation profile of the Sun and other stars are discussed. The main results of the paper are summarized in Section 5.

2 EXTRACTION OF ROTATIONAL SPLITTING FREQUENCIES

We have analyzed the p-mode rotational splittings observed by the Birmingham Solar-Oscillations Network (BiSON; Elsworth et al. 1995a; Chaplin et al. 1996) during the last two solar cycles in their entirety i.e. from 1986 April 14 to 2010 April 7. The Global Oscillations at Low Frequencies (GOLF; Gabriel et al. 1995) instrument on board the ESA/NASA Solar and Heliospheric Observatory (SOHO) spacecraft has been collecting data since 1996 and so we have been able to analyze the velocity data (following the methods described in Jiménez-Reyes et al. 2003; García et al. 2005) covering almost the entirety of solar cycle 23, i.e., from 1996 April 11 to 2010 April 7.

The precision with which p-mode parameters, such as the rotational splittings, can be determined is directly related to the length of data set under consideration. Consequently, p-mode frequencies are often determined from data sets whose lengths are of the order of years. However, a compromise must be made here regarding the appropriate length of data set for study so that changes as the solar cycle evolves can be resolved. Therefore the observations made by GOLF and BiSON were divided into 182.5-day-long independent subsets. After 1996 April 11, when both sets of data were available, we ensured that the start times of the subsets from each observational program were the same.

Estimates of the mode splittings were extracted from each subset by fitting a modified Lorentzian model to the data using a standard likelihood maximization method, where the rotational splitting was a free parameter in the model.

The unweighted mean mode splitting for a particular subset was then determined by averaging estimates in the frequency range 2000 – 3100 μHz. The lower limit of this frequency range (i.e., 2000 μHz) was the lowest frequency for which the signal-to-noise value allowed good fits to be obtained in all the subsets. Furthermore, below this frequency the mode frequencies experience almost no solar cycle shift (e.g. Libbrecht & Woodard 1990; Elsworth et al. 1994). Above 3100 μHz it becomes difficult to accurately determine the mode splittings as the widths of the modes become larger than the splitting itself and so the mode components overlap in frequency, eventually becoming a single peak. The mean splittings were calculated for the $l = 1$ and $l = 2$ modes separately.

Table 1. Pearson's and Spearman's rank correlations between the BiSON and GOLF splittings

	$l = 1$	$l = 2$
Pearson's	0.84	0.63
Spearman's	0.80	0.63

Two different fitting codes have been used to extract the mode frequencies (Salabert et al. 2007; Fletcher et al. 2009), both giving similar results. For GOLF the mean absolute difference in the estimated average splittings was 0.3σ for $l = 1$ and 0.4σ for $l = 2$, and the difference in the estimated splittings from the two codes was always within 1σ. For BiSON, the mean absolute difference in the estimated splittings was 0.5σ for $l = 1$ and 0.6σ for $l = 2$. Differences in the way the fitting procedures dealt with the BiSON window function meant that before 1992, when the BiSON duty cycle was often below 50 per cent, the splittings obtained from the BiSON data were separated by up to 3σ. However, after 1992 the maximum separation of the BiSON splittings obtained by the two different fitting methods was 1.1σ. For clarity, we only show the results of one method, which is described in Fletcher et al..

Many authors have examined the uncertainties associated with estimating splittings from Sun-as-a-star observations and the biases associated with the estimated splittings are now well known (e.g. Eff-Darwich & Korzennik 1998; Appourchaux et al. 2000; Chaplin et al. 2006; García et al. 2008). We follow the advice of Chaplin et al. (2006) in order to minimize these biases. For example, Chaplin et al. found that one of the main sources of bias in estimated splittings arises if the amplitude ratios of the m components inside a multiplet are not set correctly. We therefore fix these ratios at previously determined and accepted values for BiSON and GOLF (Chaplin et al. 2006; Salabert, Ballot & García 2011). Furthermore, the amplitude of the majority of known systematic errors become appreciable above approximately 3400 μHz, which is above the upper limit on the frequency range we examine here.

2.1 Variation with time of the rotational splitting frequencies

Let us now consider whether the rotational splitting measured with the methodology outlined above show any significant variations with time. Fig. 1 shows the mean determined splittings as a function of time, $a_l(t)$, for GOLF and BiSON. There is no obvious evidence for an 11-yr solar cycle effect on the splittings. This is consistent with previous results (e.g. Jiménez, Roca Cortés & Jiménez-Reyes 2002; Gelly et al. 2002; García et al. 2004, 2008; Salabert et al. 2011a). However, there are discernible mid-term ($\sim$ 2 yr) variations, which is also in agreement with the results of Salabert et al. (2011a). There is significant correlation between the variations in the splittings observed in the two data sets (see Table 1), such that there is less than a 0.05 per cent probability of the correlations occurring by chance.

There is no correlation between the $l = 1$ and $l = 2$ mode splittings for either the GOLF or the BiSON data. The splittings of the $l = 1$ modes show more variation than the $l = 2$ mode splittings. This is not surprising and indicates that, in Sun-as-a-star data, the rotational splittings estimated from $l = 2$ modes are more stable than the splittings estimated using $l = 1$ modes (see e.g. Chaplin et al. 2006). However, as we now show, this difference is accounted for by the formal uncertainties associated with the estimated splittings. We define $\bar{a_l}$ to be the temporal mean of $a_l(t)$ and $\delta a_l(t) = a_l(t) - \bar{a_l}$. Fig. 2, which

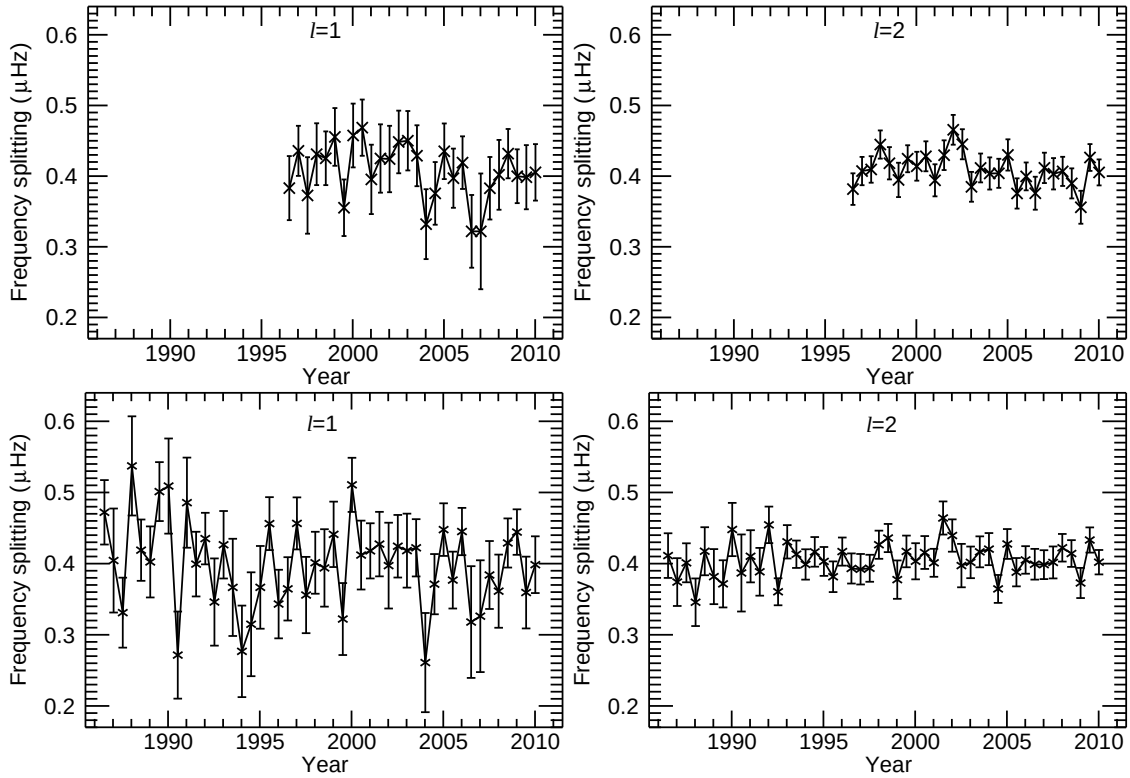

Figure 1. Mean splittings observed in GOLF and BiSON data. The top panels show the results found using the GOLF data and the bottom panels show the BiSON results. The left-hand panels show the $l = 1$ results and the right-hand panels show the $l = 2$ results.

Table 2. Standard deviation of the error normalized residuals (plotted in Fig. 2).

l	GOLF	BiSON
1	0.82	1.14
2	1.07	1.00

shows $\delta a_l(t)/\sigma_a$ (where σ_a is the formal uncertainty associated with $a_l(t)$), demonstrates that the scatter in the plots is similar for $l = 1$ and 2, indicating that the relative variation in the splittings is comparable. Table 2 gives the standard deviations of the error normalized residuals, $\delta a_l(t)/\sigma_a$. The standard deviations of the normalized residuals are close to unity for both GOLF and BiSON data, which is what we would expect to observe for a totally random process with appropriate error bars.

2.2 Periodograms of the observed splittings

To further investigate whether the observed variations are significant, we computed periodograms of the observed splittings. These periodograms are plotted in Fig. 3. In calculating the periodograms the data have been oversampled by a factor of 10. The cut-off frequency at the low end of the periodograms, below which no information can be obtained, is $0.07\,\mathrm{yr}^{-1}$ and $0.042\,\mathrm{yr}^{-1}$ for GOLF and BiSON respectively. Also plotted in Fig. 3 are the 1 per cent false alarm significance levels (Chaplin et al. 2002), which were determined using Monte Carlo simulations. 200,000 noise data sets were simulated, using a normal distribution random number generator, to mimic those plotted in Fig. 1. The standard deviation of each point on the data set was taken as the 1σ uncertainty associated with the rotational split-

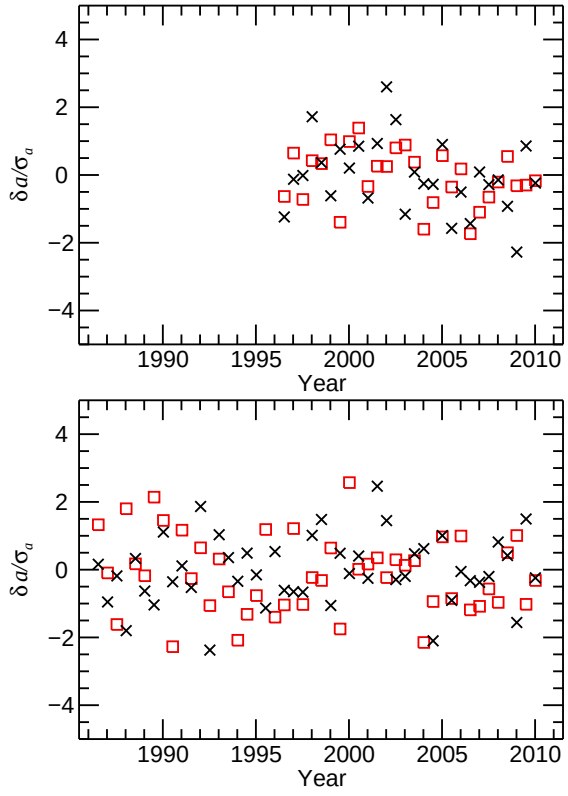

Figure 2. Relative variation in the error normalized residuals, $(\delta a_l(t)/\sigma_a)$. The top panel shows the results for GOLF and the bottom panel shows the results for BiSON. The red squares show the $l = 1$ results and the black crosses show the $l = 2$ results.

Table 3. Null probability of observing the peaks in the BiSON periodogram (Fig. 3) in noise.

l	Frequency (yr^{-1})	Probability (%)
1	0.08	0.190
1	0.58	0.797
1	0.67	0.679
2	0.92	0.337

tings plotted in Fig. 1. The simulated data sets were then used to create periodograms and the amplitudes observed in the simulated periodograms were used to define the 1 per cent false alarm significance levels. The 1 per cent significance level is somewhat arbitrary, but was chosen a priori so that the number of expected false detections is less than unity (see e.g. Chaplin et al. 2002; Broomhall et al. 2010).

There are no significant peaks (at a 1 per cent level) in the periodogram of the GOLF data indicating that there are no significant periodicities in the GOLF rotational splittings. However, there are three significant peaks in the $l = 1$ BiSON periodogram and one significant periodicity in the BiSON $l = 2$ splittings. The significant peak in the BiSON $l = 2$ periodogram (at $\sim 0.92\,yr^{-1}$) does not correspond to any of the significant peaks in the BiSON $l = 1$ periodogram.

Table 3 contains the probabilities of those peaks in the BiSON periodogram where the probability of observing the peaks by change is less than 1 per cent. Although two of the $l = 1$ peaks are only marginally significant the other $l = 1$ peak (at $0.67\,yr^{-1}$) and the $l = 2$ peak are well below the significance level. The uncertainties associated with the splittings would have to be increased by 10 per cent for the $l = 2$ modes and 17 per cent for the $l = 1$ modes before these peaks are no longer significant.

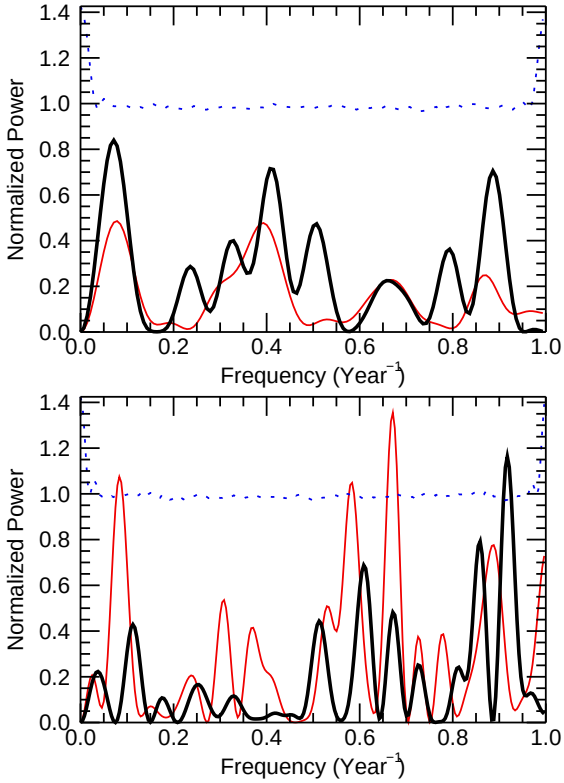

Figure 3. Periodograms of the mean splittings observed in GOLF (top panel) and BiSON (bottom panel) data. Each periodogram has been normalized so that the power is unity when the mean significance level is 1 per cent. This means that the $l = 1$ and 2 significance levels are now coincident. In each panel the red, thin line represents the $l = 1$ results, the black, thick line represents the $l = 2$ results and the blue dotted line represent the 1 per cent significance level.

3 COMPARISON WITH SOLARFLAG DATA

To help determine whether the signals observed in the BiSON data are really solar in origin (e.g. perhaps associated with the solar cycle) or simply an artifact of the data analysis procedure we examined data that were simulated for the solar Fitting at Low Angular degree Group (solarFLAG; Chaplin et al. 2006). The data were simulated in the time domain and were designed to mimic Sun-as-a-star observations. The simulated oscillations were stochastically excited and damped with lifetimes analogous to those of real solar oscillations. Five sets of solarFLAG data were examined. The input mode frequencies were the same in each simulated data set and were constant in time. The mode splittings were fixed at $0.4\,\mu$Hz. However, the data simulated the stochastic nature of the mode excitation giving access to different mode and noise realizations. The simulated data were approximately 9 yr in length but were split into subsets of 182.5 d for analysis.

The splittings obtained from a typical solarFLAG data set (FLAGa) are plotted in Fig. 4. Almost as much variation is observed in the splittings obtained from the solarFLAG data as was observed in the real data. Table 4 shows the mean observed splittings and the maximum absolute deviation from the mean for both the real and simulated data. The maximum absolute deviations of the BiSON data are slightly larger than all of the simulated solarFLAG data sets, while the GOLF data are in reasonable agreement with the solarFLAG data. Since the only source of variation in the solarFLAG data is the realization noise these results imply that the changes seen in the real data are more than likely due to realization noise.

3.1 Impact of the BiSON window function

The discrepancy between the maximum absolute deviations observed in the BiSON results and the GOLF and solarFLAG results can be explained by the impact of the window functions of the respective data sets. The duty cycles of the BiSON subsets range from 22 to 88 per cent, with the average duty cycle being 69 per cent. Normally the duty cycle of the GOLF data is above 90 per cent and the mean duty cycle is 95 per cent. However, the lowest observed duty cycle of the GOLF subsets was 42 per cent, which coincides with when control of SOHO was temporarily lost, known as the "SOHO vacation". BiSON window functions were applied to the GOLF data such that the 182.5 d BiSON subset from which the window function was extracted matched in time the GOLF subset to which it was applied. Table 4 shows that this increases the maximum absolute deviations of the GOLF data. Furthermore, although not shown here, a marginally significant peak (at a 1 per cent significance level) was observed at $\sim 0.9\,yr^{-1}$ in the periodogram of the $l = 2$ splittings.

Various BiSON window functions were also imposed on the solarFLAG data, with duty cycles covering the range observed here. In addition to the splittings observed in the 100 per cent duty cycle solarFLAG data, Fig. 4 also shows the splittings obtained from one set of solarFLAG data when a 182.5-d-long BiSON window function, with a duty cycle of 88 per cent, was imposed upon each 182.5-d-long subset. This is just one example of the window functions that were imposed. The same BiSON window function was imposed on each FLAG subset so that the average duty cycle could be varied systematically. When some window functions were imposed the maximum absolute deviations were observed to increase to values similar to those observed

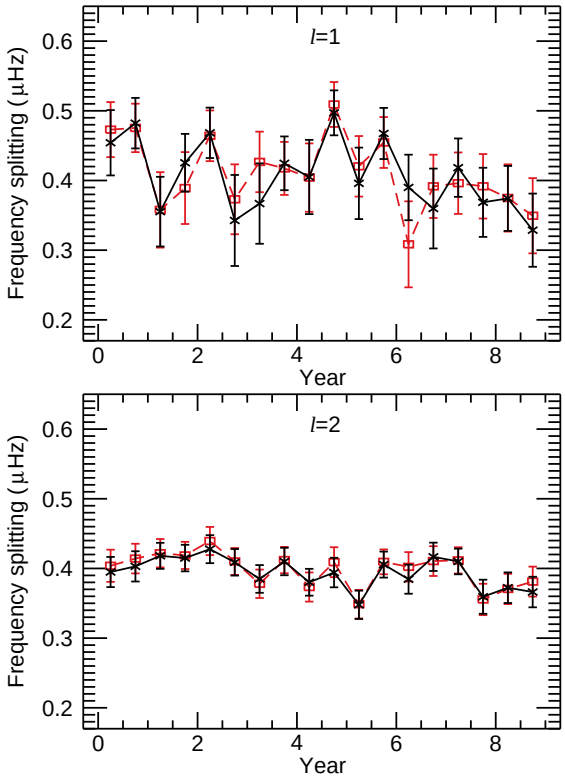

Figure 4. Mean splittings observed in one of the simulated solarFLAG data sets (FLAGa). The top panel shows the $l = 1$ results and the bottom panel shows the $l = 2$ results. The black crosses with the solid line represent the results when the solarFLAG data had a duty cycle of 100 per cent. The red squares with the dashed line represent the results when the 182.5-d-long solarFLAG subsets were given a BiSON window function with a duty cycle of 88 per cent.

in the BiSON data. However, in other cases the maximum absolute deviation was observed to decrease. Table 5 shows that, although altering the window function changes the maximum absolute deviation, the obtained deviation is not dependent on the value of the duty cycle. For example, the $l = 1$ rotational splittings observed in FLAGa varied more when the duty cycle was 88 per cent than when the duty cycle was 47 per cent.

This is consistent with the surmise that the observed variations are due to realization noise and that the window function could affect the variations in the rotational splittings both constructively and destructively via its interaction with the noise. Consider a period of time when the realization noise shifts the obtained splitting away from the true value. If the window function blanks this period of time (i.e. there is no data available) then the estimated rotational splitting will be close to the true value and the observed variation in the rotational splittings will decrease. However, the window function could equally favour times when the realization noise shifts the observed rotational splitting away from the true value. The variation in the rotational splittings will then increase.

This hypothesis is strengthened further by analysis of the periodograms of the solarFLAG data. Fig. 5 shows periodograms of the splittings obtained from the solarFLAG data sets when various BiSON window functions were imposed. We start by considering the top-left panel of Fig. 5, which shows periodograms of the $l = 1$ splittings obtained from the FLAGc data when BiSON window functions were imposed such that the duty cycle of the data was 59 per cent, 68 per cent and 76 per cent respectively. Even though the splittings included in the simulated FLAG data were constant, significant peaks (at a 1 per cent false alarm level) are observed in the periodograms. Significant peaks are observed when the duty cycle was both 59 per cent and 76 per cent but not 68 per cent. Similarly in the top middle panel of Fig. 5 significant peaks (at a 1 per cent false alarm level) are observed in periodograms of the $l = 1$ splittings obtained from the FLAGd data when the duty cycle is 68 per cent but not 47 per cent or 100 per cent. This indicates that the likelihood of observing a significant peak is not simply a function of the duty cycle. The bottom left and middle panels show that the same is true for the $l = 2$ splittings: The bottom left panel shows that significant peaks are observed in the $l = 2$ splittings obtained from the FLAGe data when the duty cycle was 39 per cent and 100 per cent but not 59 per cent. The bottom middle panel shows that significant peaks are observed in the $l = 2$ splittings obtained from the FLAGb data when the duty cycle was 76 per cent but not 47 per cent or 100 per cent. This shows that more important than the actual duty cycle itself is the manner in which the window function interacts with the realisation noise. The top and bottom right-hand panels of Fig. 5 show just how different the periodograms can look simply by changing the window function of the data.

We note here that Tables 4 and 5 indicate that the mean $l = 1$ rotational splittings are consistently higher than the input value of 0.4 μHz, because the rotationally split components overlap in frequency giving rise to a positive bias (Chaplin et al. 2006).

The results of the solar-FLAG simulations show that significant quasi-periodic variations can be observed in the splittings even when no actual, underlying variations in the splittings are present. The BiSON window function can act to both enhance or reduce the significance of the variation.

4 CONSEQUENCES FOR ROTATION PROFILE INVERSIONS

Let us examine the consequences of these apparent variations in the splittings for both helioseismic rotation inversion profiles and asteroseismic inferences of the mean internal rotation rate. Each rotational splitting is a spatially weighted average of certain volumes of a star's internal rotation rate and various inversion techniques have been developed to infer the Sun's internal rotation profile from the observed splittings. We now consider the consequences of the observed variations in the splittings on inferences that can be made about the rotation profiles of the Sun and other stars.

4.1 Inversions of the Sun's internal rotation profile

We have seen that, although the mean BiSON $l = 1$ splitting is $0.411 \pm 0.007\,\mu$Hz, the maximum and minimum observed splittings are $0.537 \pm 0.070\,\mu$Hz and $0.261 \pm 0.070\,\mu$Hz respectively. We have already shown that the observed variation in the splittings is just an artifact associated with the realization noise in the data and the process by which the data were analyzed. However, one may erroneously ascribe the splitting variations to a physical change in the rotation rate of a region of the solar interior. We have split the solar interior into 4 regions; the solar core ($0.00R_\odot \leq r < 0.20R_\odot$), the radiative zone ($0.20R_\odot \leq r < 0.70R_\odot$), the convection zone ($0.70R_\odot \leq r < 0.95R_\odot$), and the near-surface shear layer ($0.95R_\odot \leq r < 1.00R_\odot$). We have then determined by how much the rotation rate of that layer would need to change, relative to an average 2D Regularized Least Squares (RLS) inversion (Schou, Christensen-Dalsgaard & Thompson 1994) of the solar rotation profile, to explain the observed differences in the rotational splittings. The inversions (Thompson et al. 1996; Howe et al. 2005) were made using 15 yrs of Global Oscillations Network Group (GONG, Harvey et al. 1996) data. This analysis is similar to that performed for the Sun by Elsworth et al. (1995b) and more details can be found in Appendix A.

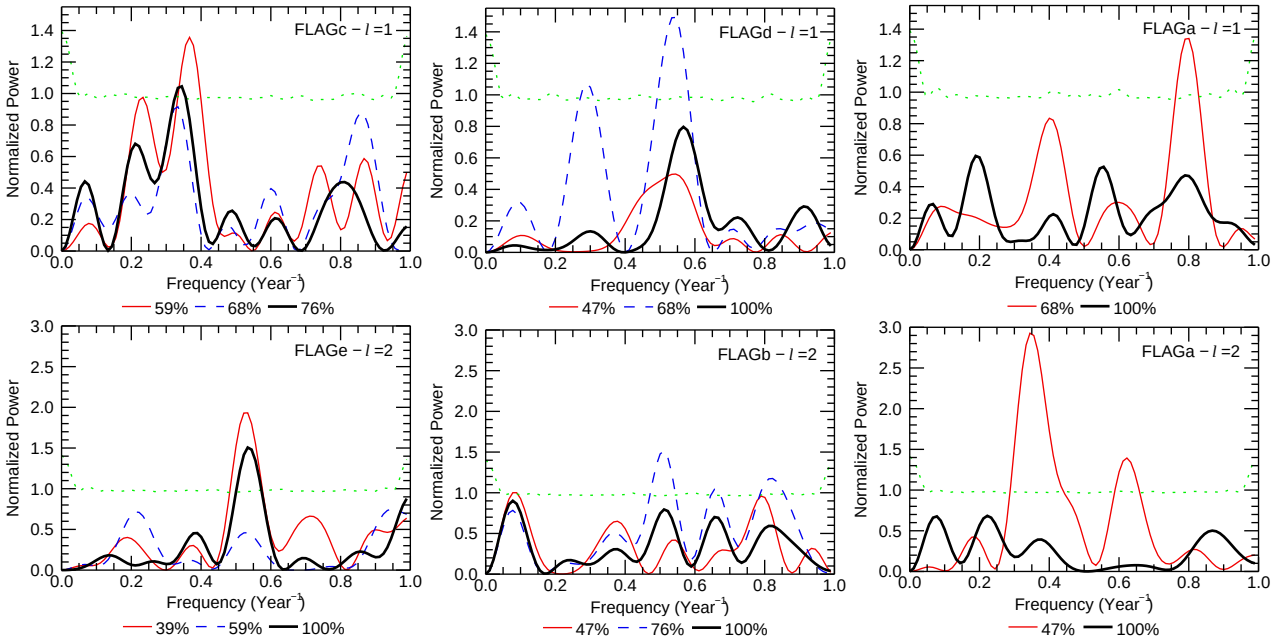

Figure 5. Periodograms of the mean splittings observed in a selection of the simulated solarFLAG data sets. The periodograms have been normalized so that the mean 1 per cent significance level (green dotted lines) is unity. The duty cycle of the BiSON window functions imposed on each subset are indicated in the legends. The top row shows $l = 1$ results, while the bottom row shows $l = 2$ results. The left and middle columns show that the power of peaks in the periodograms can both increase and decrease as the duty cycle decreases. The right-hand column shows that changes in the duty cycle can give rise to very different periodograms.

Table 4. Mean splittings and maximum absolute deviation from the mean.

Data set	Mean splitting (μHz)		Maximum absolute deviation (μHz)	
	$l = 1$	$l = 2$	$l = 1$	$l = 2$
BiSON	0.411 ± 0.007	0.406 ± 0.003	0.150 ± 0.070	0.061 ± 0.034
GOLF	0.412 ± 0.008	0.410 ± 0.004	0.090 ± 0.082	0.056 ± 0.021
GOLF (BiSON window function)	0.414 ± 0.008	0.412 ± 0.004	0.125 ± 0.073	0.068 ± 0.038
FLAGa	0.424 ± 0.010	0.396 ± 0.005	0.095 ± 0.054	0.048 ± 0.021
FLAGb	0.423 ± 0.010	0.397 ± 0.005	0.064 ± 0.053	0.059 ± 0.019
FLAGc	0.426 ± 0.010	0.406 ± 0.005	0.096 ± 0.076	0.035 ± 0.024
FLAGd	0.421 ± 0.011	0.401 ± 0.005	0.097 ± 0.077	0.042 ± 0.045
FLAGe	0.413 ± 0.010	0.408 ± 0.005	0.069 ± 0.068	0.054 ± 0.022

Table 5. Mean splittings and maximum absolute deviation from the mean estimated from the FLAGa data set when different window functions were imposed on the data.

Duty cycle (%)	Mean splitting (μHz)		Maximum absolute deviation (μHz)	
	$l = 1$	$l = 2$	$l = 1$	$l = 2$
100	0.424 ± 0.010	0.396 ± 0.005	0.095 ± 0.054	0.048 ± 0.021
88	0.426 ± 0.010	0.400 ± 0.005	0.117 ± 0.063	0.051 ± 0.021
76	0.416 ± 0.010	0.396 ± 0.005	0.110 ± 0.054	0.043 ± 0.023
68	0.435 ± 0.010	0.392 ± 0.005	0.121 ± 0.047	0.055 ± 0.024
59	0.417 ± 0.009	0.382 ± 0.005	0.103 ± 0.062	0.046 ± 0.020
47	0.421 ± 0.008	0.399 ± 0.005	0.095 ± 0.056	0.088 ± 0.023
38	0.414 ± 0.010	0.379 ± 0.006	0.130 ± 0.063	0.053 ± 0.035
22	0.406 ± 0.012	0.403 ± 0.008	0.162 ± 0.078	0.138 ± 0.029

Table 6. Variation in $\Omega/2\pi$ required to explain a $0.15\,\mu$Hz change in the rotational splitting of $l = 1$ and 2, $n = 17$ modes.

Shell	Inner radius of shell ($r/R_\odot$)	$l = 1$ (μHz)	$l = 2$ (μHz)
core	0.00	2.36	3.27
radiative zone	0.20	0.50	0.48
convection zone	0.70	0.47	0.47
surface shear layer	0.95	0.49	0.49

Using the above mentioned maximum and minimum measured splittings we find that the maximum departure from the mean BiSON splitting was $0.150 \pm 0.070\,\mu$Hz. Table 6 shows the change in rotation rate, $\mathrm{d}(\Omega/2\pi)$, required to change the observed splitting of $l = 1$ and 2, $n = 17$ modes by $0.15\,\mu$Hz (results for other modes can be found in Appendix A). The results indicate that the changes required in the rotation rate of near-surface regions to explain a difference in the splitting of $0.15\,\mu$Hz are not unreasonably large. However, observations of higher-l modes rule out variations in the near-surface regions even of this magnitude (see Appendix B). Information from higher-l modes dominate and constrain inversions of the rotation in outer regions of the solar interior at better than a 0.5 per cent level. Although variations with time in the higher-l splittings are detectable (due to the torsional oscillation) these variations are less than $0.001\,\mu$Hz (e.g. Howe, Komm & Hill 1999) and so they are approximately 100 times smaller than the deviations observed here. Large changes in the core rotation rate are required to explain the observed change in the rotational splittings. Although the required changes are so large as to be unlikely[1] such a large change cannot be ruled out with current inversions of the solar rotation profile (see Appendix B). Even low-l modes carry so little information about the conditions of the core that the uncertainties associated with any inversions are very large.

4.2 The rotation profile of a solar-type star

Asteroseismic data often consist of just a few months of observations in which only the low-l modes are visible. Thus asteroseismic data are often similar to the 182.5 d Sun-as-a-star subsets analyzed here. We note here that this analysis is relevant for main sequence stars for which no mixed modes or g modes can be detected and used to aid inferences of the internal rotation rate. Therefore it is difficult to make inversions of the internal rotation profile of a star. However, lightcurves of a star, such as those observed by CoRoT and Kepler, can show rotational modulation due to the presence of magnetic stellar activity, such as spots and active regions. The modulation of the light curve can, therefore, be used to determine the surface rotation rate of a star (e.g. Mosser et al. 2005, 2009; Mathur et al. 2010; Ballot et al. 2011), which can then be compared to the mean internal rotation rate determined from the oscillations. The sidereal rotation rate of the Sun, as estimated from the rotation of sunspots at the surface, is approximately 27 d. The mean rotation rate of the solar interior, determined from low-l rotational frequency splittings, is 28 d. However, if we were to use the extreme values of the splittings obtained from a single 182.5 d subset, similar to those available in asteroseismic studies, we would find the mean rotation rate to be either 22 ± 3 d or 44 ± 12 d. One may, therefore, erroneously conclude that the average rotation rate of the stellar interior is different to the surface rotation rate.

[1] The rotation rate in the core is not well constrained through p modes (e.g Howe 2009, and references therein)and so, in this paper, we assumed a rate similar to the rest of the radiative zone. However, we note that g modes would provide tighter constraints on the core rotation rate (García et al. 2007; Mathur et al. 2008).

5 DISCUSSION

As with previous studies, (e.g. Jiménez, Roca Cortés & Jiménez-Reyes 2002; Gelly et al. 2002; García et al. 2004, 2008; Salabert et al. 2011a), we find no 11-yr solar cycle variation in the rotational splittings. Discernible quasi-periodic mid-term (~ 2 yr) variations are present in the splittings. However, we show that these variations are due to realization noise.

Many authors have discussed the biases associated with estimating splittings from Sun-as-a-star data (e.g. Eff-Darwich & Korzennik 1998; Appourchaux et al. 2000; Chaplin et al. 2006; García et al. 2008). We have shown that, despite taking the advice of Chaplin et al. (2006), the realization noise has a larger effect on rotational splittings than accounted for by formal uncertainties, implying that the uncertainties on the fitted splittings are underestimated. The effect of the realization noise produces an erroneous apparent mid-term (~ 2 yr) signal in the observed splittings that could, potentially, look like the quasi-biennial solar-cycle related signal that is observed in the mode frequencies (Broomhall et al. 2009; Salabert et al. 2009; Fletcher et al. 2010). Although we have shown that the mid-term signal is an artifact associated with the realization noise and the data analysis process the periodicities in the splittings may be mistakenly interpreted as a physical variation in the rotation rate. Such variations are unlikely because they would require either very large changes in the core rotation or changes in the near surface that, although smaller, are ruled out through observations of higher-l modes.

It is not surprising that the splittings observed by BiSON and GOLF are highly correlated, since they both are observing the same star. In fact we expect the splittings to be correlated whether these variations are of solar origin or whether, as we have shown, they are due to realization noise. Jiménez-Reyes et al. (2004) found that there was a strong degree of correlation between numerous mode parameters, such as mode linewidths and power densities, observed in GOLF and BiSON data. They concluded that this showed that the estimated mode parameters were dominated by the same mode realization noise (the signature of stochastic excitation). Howe et al. (2006) observed that, after the solar-activity dependence had been removed from the frequencies, significant fluctuations in the frequencies were highly correlated between BiSON, GONG, and MDI data. Howe et al. explained these correlations in terms of the stochastic nature of the mode excitation, which could be interpreted as a form of realization noise. The high level of correlation observed here between the GOLF and BiSON splittings is also due to the mode realization noise. This supports the conclusion that the mode realization noise is responsible for the observed variation in the splittings, which again demonstrates how careful one needs to be, particularly when data have correlated noise sources.

Although the spurious variations do not have a significant effect on inferred rotation profiles of the Sun they could be important for any asteroseismic inferences of the average internal rotation rate of main sequence stars for which g modes and mixed modes have not been detected. Firstly because, unlike for the Sun, we must rely on the splittings estimated from low-l modes only. Secondly, because we often have only one relatively short data set, of the order of a few months, from which to extract the splittings. An additional consideration is that the accuracy of the determined splitting is dependent on the size of the splittings relative to the width of the modes i.e. whether the modes overlap in frequency (Ballot, García & Lambert 2006; Ballot et al. 2008). We have shown that care must be taken in using average splittings (extracted from data sets of a few months du-

ration) to infer the mean internal rotation rate (which, for example, might be compared in asteroseismic studies to the surface rotation rate inferred directly from rotational modulation of the light curve, e.g. Ballot et al. 2011). Artificial data, such as those available through AsteroFLAG (Chaplin et al. 2008), should be used to test for potential biases in the results. Care should be taken when interpreting the observed splittings of low-l modes in both astero- and helioseismic data.

APPENDIX A: INVERSION PROCESS: FORWARD CALCULATIONS

A rotation profile of the Sun was simulated, based on the average of 2D inversion profiles computed over 15 yrs using a Regularized Least Squares (RLS, Schou, Christensen-Dalsgaard & Thompson 1994) inversion method and Global Oscillations Network Group data (GONG, Harvey et al. 1996; Thompson et al. 1996; Howe et al. 2005). The GONG instrument make spatially resolved observations of the Sun and is thus able to observe much higher-l modes than those examined here. The GONG observations were used to build a latitudinally dependent rotation profile of the Sun between 0.5 and 1.0 solar radii ($R_\odot$). Below $0.5\,R_\odot$ the rotation was taken to be constant and equal to the mean inferred rotation rate across all latitudes at $0.5\,R_\odot$. We varied the rotation rate in four different regions of the solar interior; the solar core ($0.00R_\odot \leq r < 0.20R_\odot$), the radiative zone ($0.20R_\odot \leq r < 0.70R_\odot$), the convection zone ($0.70R_\odot \leq r < 0.95R_\odot$), and the near-surface shear layer ($0.95R_\odot \leq r < 1.00R_\odot$). The splittings were calculated when the rotation rate in each region was varied between $330 \leq \Omega/2\pi \leq 530$ nHz. The $l = 1$ and 2 splittings, $\delta\nu$, were then determined (see for example Chaplin et al. 1999).

To first order, the magnitudes of the splittings vary linearly with the rotation rate in a given region. That linear factor depends on the position of the specific region in the solar interior and so can be used to infer the change in rotation rate in a specific region that is required to produce a change in splitting of $0.15\,\mu$Hz. These values are plotted in Fig. A1 and are listed in Table 6 for $l = 1$, $n = 17$ and $l = 2$, $n = 17$ (corresponding to modes at 2561 and 2621 μHz respectively). The results in Fig. A1 and Table 6 indicate by how much the rotation rate in a particular region would have to deviate from the values obtained from the 15-yr 2D RLS inversions to explain the observed results. The required deviation in rotation rate change is similar for the radiative zone, the convection zone and the surface shear layer and is approximately constant across the range of n examined here. However, the change in rotation rate required in the core is substantially larger and depends on n.

As expected from the rotation kernels, the observed splittings are much more sensitive to surface regions than to the core. The changes in Table 6 can be compared to the mean rotation rate at the surface, which is approximately $\Omega/2\pi = 430$ nHz. The rotation rate in the core would have to be approximately 5 times faster than the mean solar surface rotation rate to account for an increase in the splitting of $0.15\,\mu$Hz, while the rotation rate in the other regions of the solar interior would have to change by more than 100 per cent of the mean solar value. In other words, even if the shell responsible for the change in splitting is close to the surface, a large, but not inconceivable, change in rotation rate is required to explain a difference in the observed splitting of $0.15\,\mu$Hz.

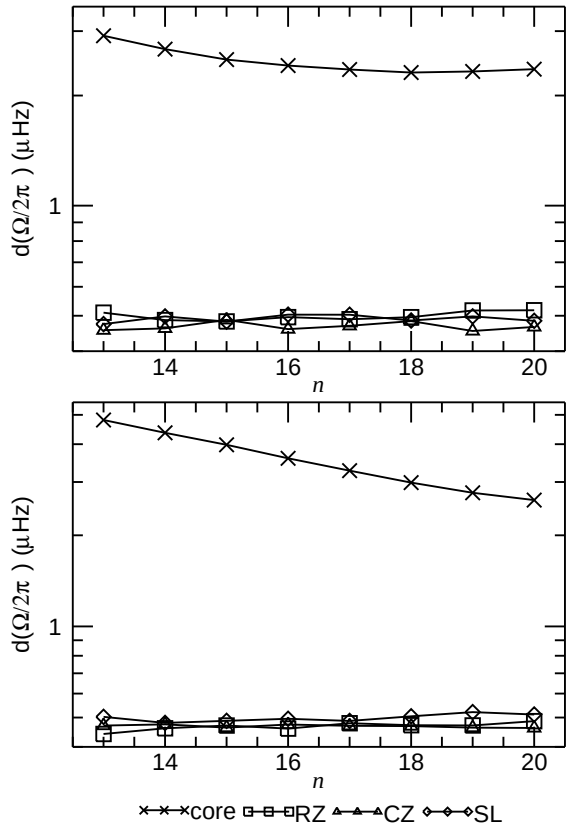

Figure A1. Change in rotation rate required to account for a $0.15\,\mu$Hz change in the observed splitting as a function of n, for $l = 1$ (top panel) and $l = 2$ (bottom panel) modes. The different symbols correspond to the results obtained when the rotation rate in a specific region was altered (see legend).

APPENDIX B: VARIATIONS IN THE INFERRED SOLAR ROTATION PROFILE

We have combined the low-degree splittings observed in the BiSON and GOLF data with a set of intermediate-degree splittings made from the average of three 72 d Michelson Doppler Imager (MDI, Scherrer et al. 1995) sets observed between 1996 and 1997. Each set of splittings was then inverted using 2D RLS methods (Schou, Christensen-Dalsgaard & Thompson 1994). Fig. B1 shows residuals in the inferred rotation profile at the equator once a mean profile has been subtracted. In regions where no information is available (i.e. the core) the 2D RLS inversion method extrapolates a solution. In these regions the averaging kernels, the functions that describe how the estimate of the solution corresponds to a spatial average of the underlying true solution, are not well localized. The rotation profiles plotted in Fig. B1 were generated using two sets of splittings measured by BiSON and GOLF. These were chosen because they correspond to epochs when the observed splitting deviates noticeably from the mean. In each case the rotation profiles differ from the mean, and from each other, in the deep interior but these differences are less than the formal uncertainties for the inversions. Therefore, the spurious changes in the observed splittings do not have a significant effect on the inferred rotation profile of the Sun. This is not entirely unexpected because even though the (model-dependent) spatial weighting functions (kernels) of low-l modes do probe the solar core, they are still more sensitive to the surface regions. Indeed, the sound speed in the deep interior is much larger than near the surface, so the time the modes dwell in the core is small relative to the outer regions.

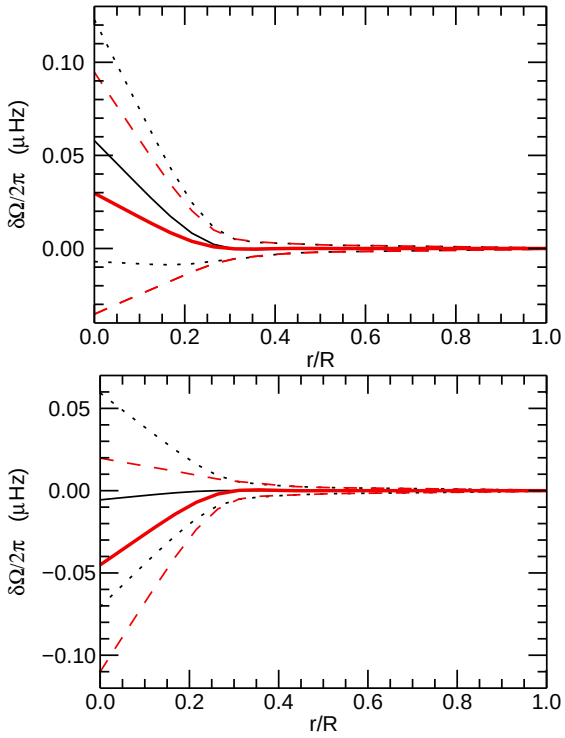

Figure B1. Residuals in the inferred profile at the equator once a mean profile was subtracted. The top panel shows the results obtained using the splittings observed in a 182.5 d subset that began on 2001 April 10 while the bottom panel shows results using the splittings observed in the 182.5 d subset that began on 2008 October 7. The black solid line shows the results obtained using the BiSON data, while the 1σ uncertainties are denoted by the black dotted lines. The red thick line shows the results obtained using the GOLF data, while the 1σ uncertainties are denoted by the red dashed lines.

ACKNOWLEDGEMENTS

We thank the referee for their insightful comments. This paper utilizes data collected by the Birmingham Solar-Oscillations Network (BiSON), which is funded by the UK Science Technology and Facilities Council (STFC). We thank the members of the BiSON team, colleagues at our host institutes, and all others, past and present, who have been associated with BiSON. The GOLF instrument on board *SOHO* is a cooperative effort of many individuals, to whom we are indebted. *SOHO* is a project of international collaboration between ESA and NASA. A.M.B., W.J.C., and Y.E. acknowledge the financial support of STFC. D.S. acknowledges the support from the Spanish National Research Plan (grant PNAyA2007-62650) and from CNES. R.A.G. thanks the support of the CNES/GOLF grant at the CEA/Saclay. R.H. thanks the National Solar Observatory for computing resources. We thank R. New for helpful comments and discussions. NCAR is supported by the National Science Foundation.

REFERENCES

Appourchaux T., Chang H.-Y., Gough D. O., Sekii T., 2000, MNRAS, 319, 365
Baglin A., Auvergne M., Barge P., Deleuil M., Catala C., Michel E., Weiss W., The COROT Team, 2006, in ESA Special Publication, Vol. 1306, ESA Special Publication, M. Fridlund, A. Baglin, J. Lochard, & L. Conroy, ed., pp. 33–+
Ballot J., Appourchaux T., Toutain T., Guittet M., 2008, A&A, 486, 867
Ballot J., García R. A., Lambert P., 2006, MNRAS, 369, 1281
Ballot J. et al., 2011, A&A, 530, A97+
Basu S., Antia H. M., 2001, MNRAS, 324, 498
—, 2003, ApJ, 585, 553
Beck P. G. et al., 2012, Nature, 481, 55
Borucki W. J. et al., 2010, Science, 327, 977
Broomhall A., Chaplin W. J., Elsworth Y., Fletcher S. T., New R., 2009, ApJL, 700, L162
Broomhall A.-M., Chaplin W. J., Elsworth Y., Appourchaux T., New R., 2010, MNRAS, 406, 767
Chaplin W. J. et al., 2008, Astronomische Nachrichten, 329, 549
—, 2006, MNRAS, 369, 985
—, 1999, MNRAS, 308, 405
—, 1996, Sol. Phys., 168, 1
Chaplin W. J., Elsworth Y., Isaak G. R., Marchenkov K. I., Miller B. A., New R., Pinter B., Appourchaux T., 2002, MNRAS, 336, 979
Chaplin W. J., Elsworth Y., Miller B. A., Verner G. A., New R., 2007, ApJ, 659, 1749
Chaplin W. J. et al., 2011, Science, 332, 213
Deheuvels S. et al., 2012, in preparation
Eff-Darwich A., Korzennik S. G., 1998, in ESA Special Publication, Vol. 418, Structure and Dynamics of the Interior of the Sun and Sun-like Stars, S. Korzennik, ed., pp. 685–+
Elsworth Y., Howe R., Isaak G. R., McLeod C. P., Miller B. A., New R., Speake C. C., Wheeler S. J., 1994, ApJ, 434, 801
Elsworth Y., Howe R., Isaak G. R., McLeod C. P., Miller B. A., New R., Wheeler S. J., 1995a, A&AS, 113, 379
Elsworth Y., Howe R., Isaak G. R., McLeod C. P., Miller B. A., New R., Wheeler S. J., Gough D. O., 1995b, Nature, 376, 669
Elsworth Y., Howe R., Isaak G. R., McLeod C. P., New R., 1990, Nature, 345, 322
Fletcher S. T., Broomhall A., Salabert D., Basu S., Chaplin W. J., Elsworth Y., García R. A., New R., 2010, ApJL, 718, L19
Fletcher S. T., Chaplin W. J., Elsworth Y., New R., 2009, ApJ, 694, 144
Gabriel A. H. et al., 1995, Sol. Phys., 162, 61
García R. A. et al., 2004, Sol. Phys., 220, 269
García R. A., Mathur S., Ballot J., Eff-Darwich A., Jiménez-Reyes S. J., Korzennik S. G., 2008, Sol. Phys., 251, 119
García R. A., Mathur S., Salabert D., Ballot J., Régulo C., Metcalfe T. S., Baglin A., 2010, Science, 329, 1032
García R. A. et al., 2005, A&A, 442, 385
García R. A., Turck-Chièze S., Jiménez-Reyes S. J., Ballot J., Pallé P. L., Eff-Darwich A., Mathur S., Provost J., 2007, Science, 316, 1591
Gelly B., Lazrek M., Grec G., Ayad A., Schmider F. X., Renaud C., Salabert D., Fossat E., 2002, A&A, 394, 285
Harvey J. W. et al., 1996, Science, 272, 1284
Howe R., 2009, Living Reviews in Solar Physics, 6, 1
Howe R., Chaplin W. J., Elsworth Y., Hill F., Komm R. W., Isaak G. R., New R., 2006, MNRAS, 369, 933
Howe R., Christensen-Dalsgaard J., Hill F., Komm R., Schou J., Thompson M. J., 2005, ApJ, 634, 1405
Howe R., Christensen-Dalsgaard J., Hill F., Komm R., Schou J., Thompson M. J., Toomre J., 2007, Advances in Space Research, 40, 915
Howe R., Christensen-Dalsgaard J., Hill F., Komm R. W., Larsen R. M., Schou J., Thompson M. J., Toomre J., 2000, Science, 287, 2456
Howe R., Komm R., Hill F., 1999, ApJ, 524, 1084
Jiménez A., Roca Cortés T., Jiménez-Reyes S. J., 2002, Sol. Phys., 209, 247
Jiménez-Reyes S. J., Chaplin W. J., Elsworth Y., García R. A., 2004,

ApJ, 604, 969
Jiménez-Reyes S. J., Chaplin W. J., Elsworth Y., García R. A., Howe R., Socas-Navarro H., Toutain T., 2007, ApJ, 654, 1135
Jiménez-Reyes S. J., García R. A., Jiménez A., Chaplin W. J., 2003, ApJ, 595, 446
Libbrecht K. G., Woodard M. F., 1990, Nature, 345, 779
Mathur S., Eff-Darwich A., García R. A., Turck-Chièze S., 2008, A&A, 484, 517
Mathur S. et al., 2010, A&A, 518, A53
Mosser B., Baudin F., Lanza A. F., Hulot J. C., Catala C., Baglin A., Auvergne M., 2009, A&A, 506, 245
Mosser B. et al., 2005, A&A, 431, L13
Pallé P. L., Régulo C., Roca Cortés T., 1989, A&A, 224, 253
Salabert D., Ballot J., García R. A., 2011, A&A, 528, A25+
Salabert D., Chaplin W. J., Elsworth Y., New R., Verner G. A., 2007, A&A, 463, 1181
Salabert D., Fossat E., Gelly B., Kholikov S., Grec G., Lazrek M., Schmider F. X., 2004, A&A, 413, 1135
Salabert D., García R. A., Pallé P. L., Jiménez A., 2011a, Journal of Physics Conference Series, 271, 012030
Salabert D., García R. A., Pallé P. L., Jiménez-Reyes S. J., 2009, A&A, 504, L1
Salabert D., Jiménez-Reyes S. J., Tomczyk S., 2003, A&A, 408, 729
Salabert D., Régulo C., Ballot J., García R. A., Mathur S., 2011b, A&A, 530, A127+
Scherrer P. H. et al., 1995, Sol. Phys., 162, 129
Schou J., Christensen-Dalsgaard J., Thompson M. J., 1994, ApJ, 433, 389
Thompson M. J. et al., 1996, Science, 272, 1300
Woodard M. F., Noyes R. W., 1985, Nat., 318, 449